Electron-Capture Decay of Bi^{207}: L-Subshell Fluorescence Yields and Coster-Kronig Transition Probabilities of Pb†

P. VENUGOPALA RAO, R. E. WOOD, AND J. M. PALMS
Department of Physics, Emory University, Atlanta, Georgia 30322
AND
R. W. FINK
School of Chemistry, Georgia Institute of Technology, Atlanta, Georgia 30332

(Received 16 September 1968)

Coincidence spectrometry with high-resolution Si(Li) and Ge(Li) x-ray spectrometers (resolutions 470-eV full width at half-maximum at 14.4 keV) has been employed to study directly the x rays emitted during the filling of each of the three L-subshell primary vacancies in the electron-capture decay of Bi^{207}. The L x rays, observed in the Si(Li) detector, in fast coincidence ($2\tau=110$ nsec) with $K_{\alpha 1}$ x rays detected in the Ge(Li) detector, arise entirely from initial vacancies in the L_3 subshell, while those in coincidence with $K_{\alpha 2}$ x rays are from initial L_2-subshell vacancies. The clear presence of L_α x rays, which arise only from L_3 vacancies, in the latter spectrum indicates that Coster-Kronig transitions of the type L_2-L_3X take place. The L x rays in coincidence with 1770-, 1063-, and 570-keV γ rays and with 1063-keV L-conversion electrons give information on L_1-subshell quantities. The following results are obtained: $\omega_3=0.315\pm0.013$, $\omega_2=0.363\pm0.015$, $\omega_1=0.07\pm0.02$, $\nu_1=0.295\pm0.010$, $\nu_2=0.417\pm0.015$, $f_{12}=0.15\pm0.04$, $f_{13}=0.57\pm0.03$, and $f_{23}=0.164\pm0.016$ at $Z=82$.

I. INTRODUCTION

A KNOWLEDGE of how L-subshell vacancies are filled is of particular importance in studies of radioactive processes (e.g., electron capture, internal conversion) and of ionization cross sections (from characteristic x-ray emission in charged-particle bombardment and in photoelectric processes). As the primary vacancies generally occur in all three L subshells simultaneously, the precision determination of the individual L-subshell fluorescence yields, Auger yields, and Coster-Kronig transition probabilities is seriously hampered.[1] Previously, coincidence techniques with proportional and scintillation counters have been used to isolate and study the filling of L_2-subshell vacancies[2] and of L_3 vacancies.[3,4] Recent advances in ultra-high-resolution cooled Si(Li) and Ge(Li) x-ray spectrometers [resolutions typically 400–500 eV full width at half-maximum (FWHM) at 14.4 keV] have vastly improved the possibilities of studying individual L-subshell fluorescence and Coster-Kronig yields. Bi^{207} (30 yr) is ideally suited for the investigation of all three L subshells separately to obtain the complete set of the six quantities that describe the fate of L-subshell vacancies (ω_1, ω_2, ω_3, f_{12}, f_{13}, and f_{23}). These quantities are defined and explained in Ref. 1. The notation standardized in Ref. 1 is followed in the present work.

A. Production of L-Subshell Vacancies in Bi^{207} Decay

The decay scheme of Bi^{207} is well known.[5,6] In connection with the present work, the relative γ-ray intensities have been remeasured with several large-volume Ge(Li) detectors, in order to establish the percentage branching of electron capture (EC) accurately to the levels in Pb^{207} (see Sec. III). There are two catagories of L-subshell vacancies in lead produced in this decay: (1) those created directly by EC and internal conversion; (2) those created by the filling of a K-shell vacancy in K_α x-ray and K Auger electron emission. In Table I are listed the relative distribution of *primary* L-subshell vacancies $N_1:N_2:N_3$ produced by the various processes, where $N_1+N_2+N_3=1$.

Primary vacancies created by electron capture are computed from theory[7] for the ratios of L-subshell capture probabilities P_{L_i} and of K-shell capture probability P_K. The P_L/P_K ratios are in agreement with experiment within 2% in the high-Z region.[8] The L vacancies produced in the internal conversion of the 1063-keV $M4$ transition and of the 570-keV $E2$ transi-

† Supported in part by a Research Corporation grant to Emory University and by the U.S. Atomic Energy Commission at Georgia Institute of Technology.

[1] R. W. Fink, R. C. Jopson, Hans Mark, and C. D. Swift, Rev. Mod. Phys. **38**, 513 (1966).

[2] P. Venugopala Rao and B. Crasemann, Phys. Rev. **139**, 1926 (1965).

[3] R. C. Jopson, J. M. Khan, C. D. Swift, and M. A. Williamson, Phys. Rev. **133**, A381 (1964).

[4] R. E. Price, Hans Mark, and C. D. Swift, Phys. Rev. **176**, 1 (1968); University of California Lawrence Radiation Laboratory Report No. UCRL-71058, 1968 (report of work prior to publication).

[5] *Nuclear Data Sheets*, compiled by K. Way *et al.* (Printing and Publishing Office, National Academy of Sciences–National Research Council, Washington, D.C. 20025).

[6] C. M. Lederer, J. M. Hollander, and I. Perlman, *Table of Isotopes* (John Wiley & Sons, Inc., New York, 1967), 6th ed.

[7] The L-subshell capture ratios $P_{L1}:P_{L2}:P_{L3}$ are taken from H. Brysk and M. E. Rose, Rev. Mod. Phys. **30**, 1169 (1958); Oak Ridge National Laboratory Report No. ORNL-1830, 1955 (unpublished); and from L. N. Zyryanova, in *Once-forbidden Beta-transitions*, transl. by P. Basu (Pergamon Press, Inc., London, 1963). The capture ratios P_L/P_K are taken from the recent theoretical calculations, based on new sets of wave functions, of H. Behrens and W. Bühring and of L. N. Zyryanova and Suslov, in *Proceedings of the International Conference on Electron Capture and Higher Order Processes in Nuclear Decay* (Kultura Bookexport, Budapest, Hungary, 1968).

[8] R. W. Fink, Nucl. Phys. **A110**, 379 (1968); in *Proceedings of the International Conference on Electron Capture and Higher Order Processes in Nuclear Decay* (Kultura Bookexport, Budapest, Hungary, 1968); B. L. Robinson and R. W. Fink, Rev. Mod. Phys. **32**, 117 (1960).

TABLE I. Primary L-subshell vacancies in the decay of Bi^{207}.

Method of production	N_1	$+N_2$	$+N_3=1$
L capture to the 2339-keV level	0.920	0.080	0
$K+L$ capture to the 1663-keV level	0.276	0.283	0.441
$K+L$ capture to the 570-keV level	0.241	0.296	0.463
$K_{\alpha 1}$-x-ray emission	0	0	1.0
$K_{\alpha 2}$-x-ray emission	0	1.0	0
Any K-shell vacancy[a]	0.106	0.341	0.553
L conversion of the 570-keV transition	0.531	0.346	0.123
L conversion of the 1063-keV transition	0.719	0.187	0.094

[a] Total L-subshell vacancies following a K-shell vacancy filled during $K_{\alpha 1}$, $K_{\alpha 2}$ x-ray emission or during K-LL and K-LX Auger transitions.

tion are calculated using theoretical conversion coefficients α_K and α_{L_i} from the recent tables of Hager and Seltzer.[9] The experimental conversion electron ratios K/L_1, K/L_2, K/L_3, and K-conversion coefficients for these transitions[10] agree well with the theoretical values. The L vacancies created in the K-x-ray series emission of lead are known from the relative intensities of $K_{\alpha 1}$, $K_{\alpha 2}$, and K_β x-rays given in the literature.[11]

The L vacancies following K Auger electron emission are the least well known. A critical summary of the available K Auger electron relative intensities has been given by Bergström and Nordling[12] and by Hörnfeldt.[13] The L-subshell vacancies produced in the K Auger process are calculated from the electron ratios $(K\text{-}LL):(K\text{-}LX):(K\text{-}XY)$. The K-LL intensities are taken from the smooth curves drawn through the available experimental values by Hörnfeldt.[13] The K-LX and K-XY intensities are taken from similar curves by Bergström and Nordling.[12] In spite of the fact that the Auger electron intensities are the least well-known quantities in the L-subshell primary-vacancy calculation, their contribution to the error in the present measurements is small, since fewer than about 5% of the K-shell vacancies are filled by Auger transitions.

B. Basis of the Experimental Method

The following notation is employed[14] in the equations involving counting rates. A coincidence counting rate is denoted by $C_{x(y)}$, for a coincidence spectrum of x observed with gate y. For example, $C_{L(K_{\alpha 2})}$ is the rate of L x-ray coincidences gated by $K_{\alpha 2}$ x rays; a further index on L distinguishes among L_l, L_α, L_β, L_γ x-ray components, or the particular subshell from which the L x rays arise, e.g., L_1, L_2, or L_3. The singles counting rates are denoted by a single subscript, e.g., C_γ, $C_{K_{\alpha 1}}$, etc. A double index on a subscript indicates a sum, e.g., $C_{L_{l\alpha}(K_{\alpha 1})}$ means the total coincidence counting rate of the L_l+L_α components in the coincidence spectrum gated by $K_{\alpha 1}$ x rays.

1. Study of L_1-Subshell Vacancies

L x rays arising from different primary-vacancy distributions can be observed by taking coincidences with the γ rays (1770, 1063, and 570 keV) and 1063-L-conversion electrons in Bi^{207} decay. The coincidence rate $C_{L(y)}$ is given by

$$C_{L(y)}=C_{(y)}(a_1\nu_1+a_2\nu_2+a_3\nu_3)\epsilon_L\Omega_L f_L\epsilon_c, \qquad (1)$$

where $C_{(y)}$ is the counting rate of the γ-ray or electron gating the L-x-ray spectrum; a_i are the numbers of L_1-, L_2-, and L_3-subshell vacancies in coincidence with gate y; ϵ_L and Ω_L are the counting efficiency and solid angle of the L-x-ray detector; f_L is the attenuation factor for L x rays between the source and the detector; ϵ_c is the efficiency of the fast coincidence electronic system for detecting coincidences; and ν_i is the average number of L x rays per initial L_i-subshell vacancy.

In Table II are listed the total numbers of L vacancies in each subshell in coincidence with each of the four gates employed in L_1-subshell experiments [a_i in Eqs. (9)–(12)]. These are calculated from the data on primary L vacancies from Table I, taking into account all possible coincidences with each gate. For example, in coincidence with the 1770-keV γ-ray

TABLE II. The number of L-subshell vacancies, a_i, in coincidence with each possible gate.[a]

Gate	a_1	a_2	a_3
570-keV γ ray	8.41×10^{-3}	5.28×10^{-2}	7.83×10^{-3}
1063-keV γ ray	3.95×10^{-3}	6.63×10^{-3}	8.80×10^{-3}
1770-keV γ ray	0.614	0.060	0.009
570-L-conversion electron	0.569	0.399	0.203
1063-K-conversion electron	0.106	0.335	0.541
1063-L-conversion electron	0.723	0.194	0.103

[a] In the calculation of these vacancies, theoretical conversion coefficients and electron-capture probabilities in Refs. 9 and 7, respectively, were used. For the 1770-keV γ-ray gate, an experimental value of $P_L=0.663$ was taken from the work of DeBeer, Blok, and Blok, Physica **30**, 1938 (1964). The contribution made by L conversion of the 897-, 1442-, and 1770-keV transitions is negligible.

[9] R. S. Hager and E. C. Seltzer, Nucl. Data **A4**, 1 (1968); **A4**, 2 (1968).
[10] F. P. Brady, N. F. Peek, and R. A. Warner, Nucl. Phys. **66**, 365 (1965); V. Anderson and C. J. Christensen, *ibid.* **A113**, 81 (1968).
[11] A. H. Wapstra, G. J. Nijgh, and R. Van Lieshout, *Nuclear Spectroscopy Tables* (North-Holland Publishing Co., Amsterdam, 1959), p. 81.
[12] I. Bergström and C. Nordling, in *Alpha-, Beta-, Gamma-Spectroscopy*, edited by K. Siegbahn (North-Holland Publishing Co. Amsterdam, 1964), Vol. 2, p. 1523ff.
[13] O. Hörnfeldt, Arkiv Fysik **23**, 235 (1962).
[14] P. Venugopala Rao, in *Proceedings of the International Conference on Electron Capture and Higher Order Processes in Nuclear Decay* (Kultura Bookexport, Budapest, Hungary, 1968).

gate, L vacancies are present not only from L-capture feeding of the 2339-keV level, but also from conversion of the 570-keV transition. Similarly, L x rays in coincidence with the 570-keV γ-ray gate arise from EC to the 570-keV level, conversion of the 1063- and 1770-keV transitions, and EC to the 2339-keV level. The level at 1633 keV, which is deexcited by a 1063-keV transition, is a long-lived isomeric state (0.8 sec). This fact reduces the number of L vacancies in prompt coincidence with the 1063-keV γ rays. Therefore, the only coincident L vacancies come from conversion of the 570-keV transition. Similar considerations are employed in calculating the L vacancies in coincidence with the conversion electron gates. With this knowledge of the a_i's, and the experimentally determined values of ν_2 and ν_3, Eq. (1) permits the determination of ν_1, the average number of L x rays per L_1-subshell vacancy.[1]

2. Study of L_2-Subshell Vacancies

The principle employed to study the L_2 vacancies is essentially that of Rao and Crasemann,[2] where L x rays in coincidence with $K_{\alpha 2}$ x rays are studied. The $K_{\alpha 2}$ x ray is due to the K-L_2 transition and thus always leads to an L_2-subshell vacancy. The number of (L x ray)($K_{\alpha 2}$ x ray) coincidences are given by

$$C_{L(K_{\alpha 2})}=C_{(K_{\alpha 2})}\nu_2\epsilon_L\Omega_L f_L\epsilon_c, \tag{2}$$

where $C_{(K_{\alpha 2})}$ is the number of $K_{\alpha 2}$ x rays gating the L-x-ray spectrum, and ν_2 is the average number of L x rays coming from the filling of an L_2-subshell vacancy and is expressed[1] in terms of ω_2, ω_3, and f_{23} as

$$\nu_2=\omega_2+f_{23}\omega_3. \tag{3}$$

The ratio of the intensities of L_γ to L_β components in L-x-ray spectra, observed in coincidence with $K_{\alpha 2}$ x rays, is defined as

$$s_2=C_{L_\gamma(K_{\alpha 2})}/[C_{L_\beta(K_{\alpha 2})}-s_3C_{L_{1\alpha}(K_{\alpha 2})}], \tag{4}$$

where

$$s_3=C_{L_\beta(K_{\alpha 1})}/C_{L_{1\alpha}(K_{\alpha 1})}. \tag{5}$$

Here s_2 and s_3 are the relative intensities of the respective L-x-ray components arising directly from L_2- and L_3-subshell vacancies. If $C_{L_{1\alpha}}$ is known, the total number of L x rays arising from L_3-subshell vacancies is given by

$$C_{L3}=C_{L_{1\alpha}}(1+s_3). \tag{6}$$

3. Study of L_3-Subshell Vacancies

Since the $K_{\alpha 1}$ x ray arises from the K-L_3 transition, it signals the formation of an L_3-subshell vacancy. The L_3-subshell fluorescence yield, ω_3, is related to the number of (L x ray)($K_{\alpha 1}$ x ray) coincidences by the equation

$$C_{L(K_{\alpha 1})}=C_{(K_{\alpha 1})}\omega_3\epsilon_L\Omega_L f_L\epsilon_c. \tag{7}$$

4. Determination of Coster-Kronig Transition Probabilities

The above three coincidence experiments do not require high-resolution detection of the L x rays in order to determine the quantities ν_1, ν_2, ω_3, high resolution being necessary only for the K_α x rays. However, by observing the L-x-ray spectra with resolution sufficient to resolve clearly the L_l, L_α, L_β, L_γ, etc., components in the L-x-ray series (see Fig. 1), more detailed information is obtained. The radiative transitions from the filling of an L_3 vacancy fall mainly into the L_α- and L_β-x-ray groups, which are separated by some 2 keV in lead, the L_α group being the more intense one. The L_β and L_γ groups also contain all of the transitions from L_1- and L_2-subshell vacancies. It is clear that the presence of L_l and L_α components in the coincidence spectra of L_1- and L_2-vacancy studies are related to the Coster-Kronig transition probabilities f_{12}, f_{13}, and f_{23}. The fraction of L_l+L_α x rays in these coincidence L-x-ray spectra, if carefully determined, yields an independent determination of the Coster-Kronig transition probabilities.

Determination of f_{23}. If the resolved L-x-ray spectrum in coincidence with $K_{\alpha 2}$ x rays contains L_l and L_α components, in addition to L_β and L_γ x rays which are typical of L_2 vacancies, then one concludes that some of the L_2 vacancies have been shifted by Coster-Kronig transitions to the L_3-subshell. The Coster-Kronig transition probability f_{23} is then given by the relation

$$f_{23}=[C_{(K_{\alpha 1})}/C_{(K_{\alpha 2})}][C_{L_3(K_{\alpha 2})}/C_{L(K_{\alpha 1})}]. \tag{8}$$

The only errors present in the determination of f_{23} are the statistical errors in the counting rates.

Determination of ω_1, f_{12}, *and* f_{13}. Similarly, if L x rays in coincidence with the y gates (1770-, 1063-, and 570-keV γ rays and 1063-L-conversion electrons) are resolved to obtain the intensity sum of the L_l+L_α x rays, which originate only in the L_3 subshell, one can write the following equations:

$$C_{L_3(y)}=C_{(y)}[a_1(f_{13}+f_{12}f_{23})+a_2f_{23}+a_3]\times\omega_3\epsilon_L\Omega_L f_L\epsilon_c, \tag{9}$$

$$[C_{L_{\beta\gamma}(y)}-s_3C_{L_{1\alpha}(y)}]=C_{(y)}[a_1(\omega_1+f_{12}\omega_2)+a_2\omega_2]\times\epsilon_L\Omega_L f_L\epsilon_c. \tag{10}$$

These two equations determine values of the two quantities ($f_{13}+f_{12}f_{23}$) and ($\omega_1+f_{12}\omega_2$).

If the coincidence rates of the L_β and L_γ-x-ray groups are measured separately, one can use the following two relationships to obtain values of f_{12}, f_{13}, and ω_1:

$$[C_{L_\beta(y)}-s_3C_{L_{1\alpha}(y)}]=C_{(y)}\left[\frac{a_1\omega_1}{1+s_1}+\frac{a_1\omega_2f_{12}}{1+s_2}+\frac{a_2\omega_2}{1+s_2}\right]\times\epsilon_L\Omega_L f_L\epsilon_c, \tag{11}$$

$$C_{L_\gamma(y)}=C_{(y)}\left[\frac{a_1s_1\omega_1}{1+s_1}+\frac{a_1s_2\omega_2f_{12}}{1+s_2}+\frac{a_2s_2\omega_2}{1+s_2}\right]\epsilon_L\Omega_L f_L\epsilon_c, \tag{12}$$

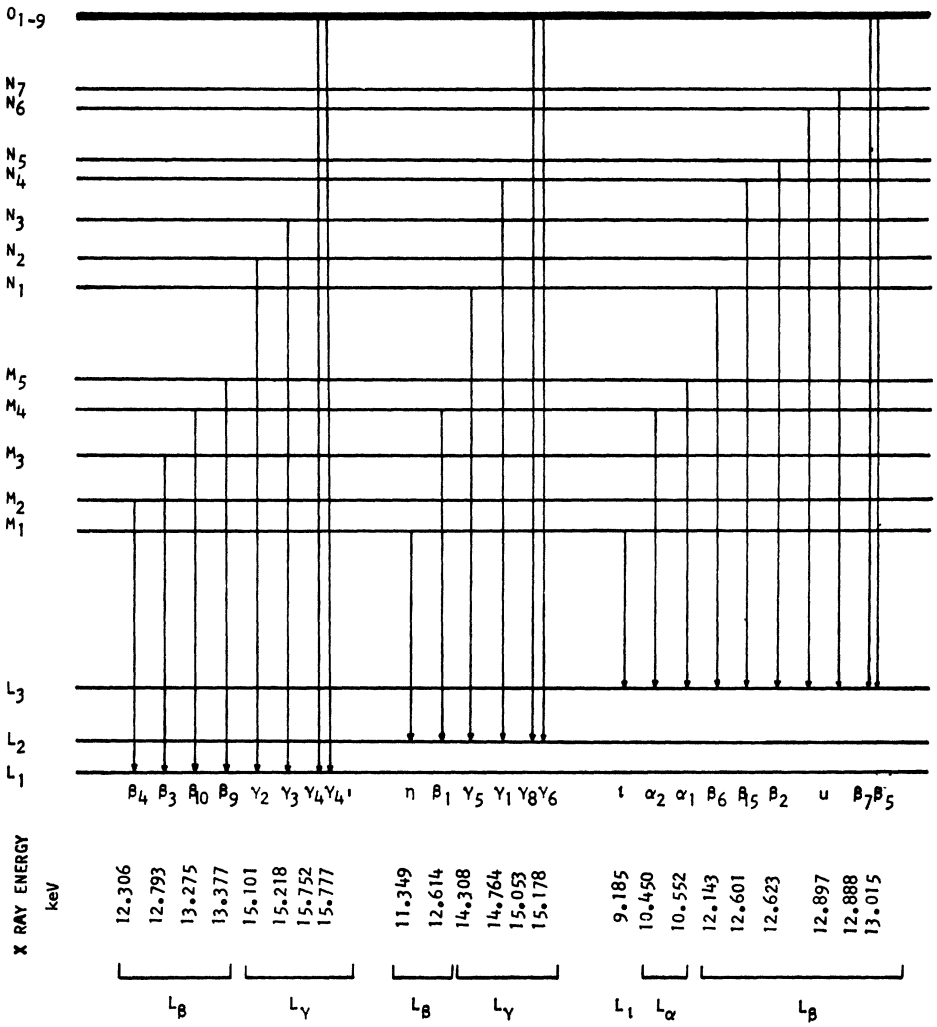

FIG. 1. The major L-series lines emitted during the filling of L_1-, L_2-, and L_3-subshell vacancies are shown. They are grouped into L_l, L_α, L_β, and L_γ components that can be resolved by existing high-resolution semiconductor detectors. It is to be noted that the L_l and L_α components are characteristic of the L_3 subshell only.

where s_1 is the ratio of intensities of the L_γ to L_β-x-ray components in the L x rays arising from the L_1 subshell and is obtained from the literature.[15]

There is a specific advantage in using (L x ray)(ce$^-$) coincidence results, instead of (L x ray)(γ) coincidences, in obtaining L_1-subshell information. The latter method makes use of assumed quantities, such as EC probabilities and conversion coefficients, in evaluating the total number of coincident L-shell vacancies. The results thus do not constitute independent information. On the other hand, if one uses (L x ray)(ce$^-$) coincidences, each conversion electron gate counts an L-shell vacancy, provided that L-conversion electrons are resolved from $M+N+\cdots$ electrons.

II. EXPERIMENTAL

A. Radioactive Sources

Carrier-free sources of 0.1 and 1.0 μCi strengths were made by evaporating a small drop of Bi^{207} in dilute HNO_3 on Mylar and Lucite backings and covering with a thin film ($\approx$100 μg/cm^2) of Krylon acrylic spray. For use as electron sources, a 20 μCi uncovered Bi^{207} source on Mylar backing was used.

B. Detectors

1. *Si(Li) X-Ray Detector*

An ORTEC Series 7110 Si(Li) x-ray detector having an active diameter of 8 mm and sensitive depth of 1.8 mm was employed to observe L x rays. The input stage of the preamplifier is encapsulated with the detector and operated at liquid-nitrogen temperature to minimize electrical noise. The window of the detector system is 0.25-mm Be plate with a few-Å-thick layer of aluminum evaporated onto its inner side. The resolution is about 600-eV FWHM at 14.4 keV, sufficient to resolve L_l, L_α, L_β, and L_γ components in the Pb L-x-ray spectrum. The intrinsic photopeak efficiency (ϵ_L) of the Si(Li) detector is essentially unity for Pb L x rays (10.5–16 keV). The attenuation

[15] M. Goldberg, Ann. Phys. (Paris) 7, 329 (1962).

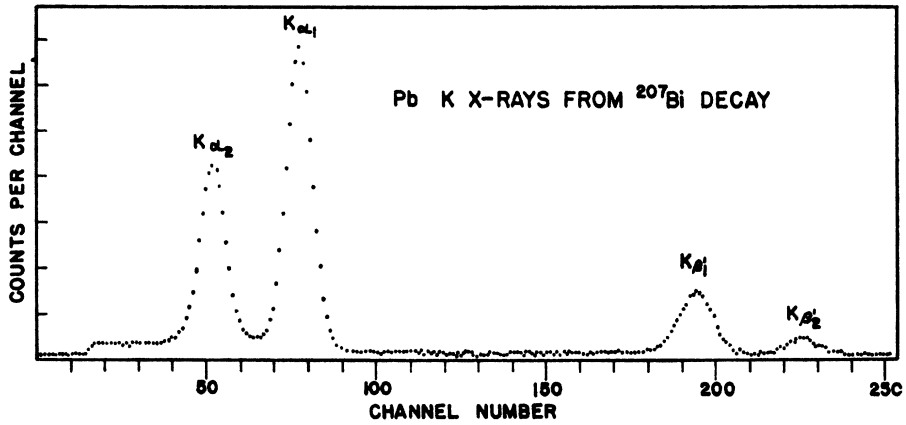

FIG. 2. Pb K x rays from Bi^{207} decay taken with a Ge(Li) x-ray spectrometer having resolution of 470-eV FWHM at 14.4 keV.

factor (f_L) due to air, Be window, and other materials present between source and active volume of the detector are calculated from x-ray attenuation coefficients in the literature.[16] The other materials include the Al layer on the Be window, a possible dead layer of Si in the detector, and $\approx$200 Å of gold for electrical contact on the detector surface. An equivalent thickness of Al was estimated by comparing the ratio of intensities of Fe K x rays to 14.4-keV γ rays from a calibrated source of Co^{57}, in order to correct for the presence of these materials. The solid angle (Ω_L) subtended by the detector at each geometry is calculated by comparing the respective counting rates of each source with their calibrated absolute counting rates, as determined in a good geometry arrangement consisting of a 25.4×0.8-mm-NaI(Tl) detector, where the source was placed at a sufficiently large distance for a point-source approximation.

The Si(Li) detector also was used to observe conversion electrons from Bi^{207} in (L x ray)(ce$^-$) coincidence measurements.

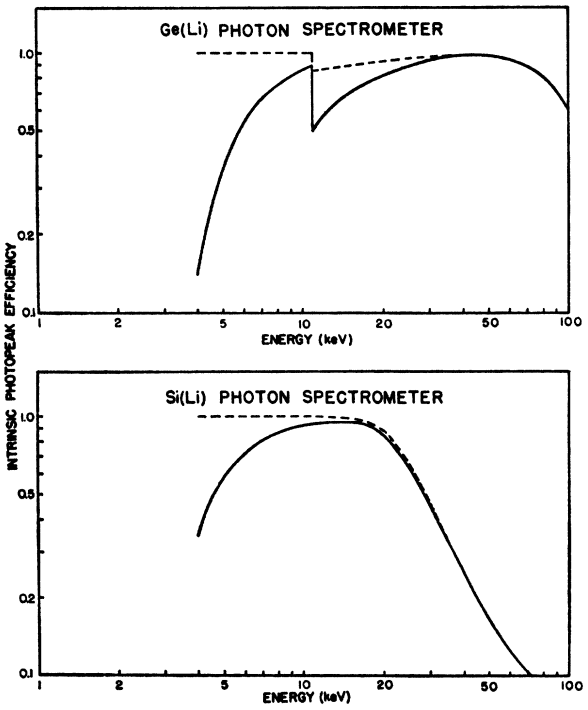

FIG. 3. The intrinsic photopeak efficiency curves for the Si(Li) and Ge(Li) x-ray spectrometers. The dashed lines are the curves for the active volumes of the detectors. The dip in the Ge(Li) detector curve at 11.1 keV is due to Ge K-x-ray escape. The solid lines include the attenuation correction due to the dead layer, gold, aluminum, and beryllium present.

2. *Ge(Li) X-Ray Detector*

The K-x-ray detector is an ORTEC Series 8010 Ge(Li) detector with diameter 8 mm and sensitive depth of 4 mm, having resolution of 470-eV FWHM at 14.4 keV. The design of the detector assembly is similar to that of the Si(Li) detector above. It has a larger detection efficiency for Pb K x rays and can resolve the $K_{\alpha 1}$, $K_{\alpha 2}$, $K_{\beta 1}$, and $K_{\beta 2}$ components (Fig. 2). In the (L x ray)(ce$^-$) coincidence experiments, this detector was used to observe the L x rays. Although the intrinsic detection efficiency of this detector in the Pb L-x-ray region is unity, the photopeak or full-energy peak efficiency is complicated by the escape of Ge K x rays ($\approx$10 keV) from the detector face. A detailed study of the escape of Ge K x rays and description of the photopeak efficiency is published elsewhere.[17] The significant point here is that the escape of Ge K x rays produces a dip in an otherwise flat photopeak efficiency curve in the energy region between the Ge K-absorption edge (11.1 keV) and 30 keV, which is just the region between the L_α and L_β x-ray components of Pb x rays. Figure 3 shows the intrinsic photopeak efficiency curves of the Si(Li) and the Ge(Li) x-ray detectors. The Ge K-x-ray escape effect is clearly demonstrated by the difference in the singles L-x-ray spectrum from Bi^{207} taken with the

[16] E. Storm and H. I. Israel, U.S. Atomic Energy Commission Report No. LA-3753, 1967 (unpublished).

[17] J. M. Palms, P. Venugopala Rao, and R. E. Wood, Nucl. Instr. Methods 64, 310 (1968).

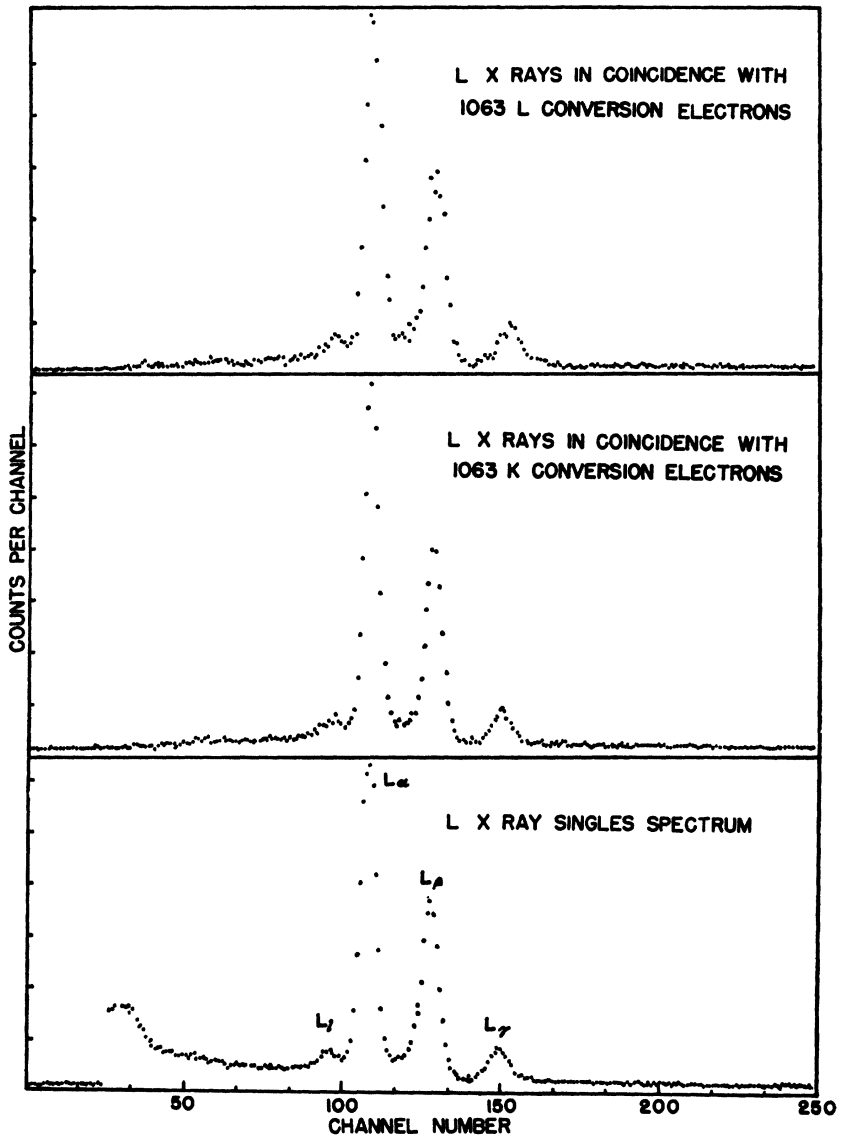

FIG. 4. Typical Pb L-x-ray spectra from Bi^{207} decay taken with Ge(Li) x-ray spectrometer. The large number of L_α x rays in coincidence with 1063-L-conversion electrons indicate that the majority of L_1-subshell vacancies are shifted to the L_3 subshell.

Ge(Li) detector, Fig. 4, and the Si(Li) detector, Fig. 5.

A conventional 7.6×7.6-cm Harshaw-integral-line NaI(Tl) detector was used to observe the γ-ray spectrum in (L x ray)(γ) coincidence measurements. In addition, large volume Ge(Li) detectors (16 and 4 cc) with resolutions of 3.5-keV FWHM at 1332 keV were used to measure the relative intensities of γ rays in Bi^{207} decay.

C. Coincidence Arrangement

An ORTEC fast coincidence system was employed in the following series of coincidence experiments, and a block diagram is shown in Fig. 6. The time-to-pulse-height converter, together with a single-channel analyzer (SCA), formed a coincidence system with variable resolving times. The resolving time was selected by changing the position of the SCA window, and a value of $2\tau = 110$ nsec was used. The upper-level discriminator and the subsequent timing signal generator, indicated by the dotted line in Fig. 6, served only to prevent distortion of the cable curve by overloading pulses from the L-x-ray detector. The chance coincidence rates were measured by introducing an additional delay in the gating channel. A detailed description of the coincidence system is being reported.[18]

A timing SCA window selected the gating K x ray, γ ray, or conversion electron in coincidence with which

[18] J. M. Palms, P. Venugopala Rao, and R. E. Wood, in *Proceedings of the Fifteenth Nuclear Science Symposium, 1968*; IEEE Trans. Nucl. Sci. NS-16, No. 1, 36 (1969).

the L-x-ray spectra were observed. The continuum due to higher-energy components in the window contributes some false L-x-ray coincidences; however, these are determined separately by shifting the window to the higher-energy side of the gate. Figure 7 shows the position of the gating window in the (L x ray)(γ) coincidence experiments to obtain the true and false coincidences. A similar procedure was adopted in the case of the (L x ray)(ce^-) and (L x ray)(K x ray) coincidence measurements.

A typical analysis of the counts observed in the gating window is presented below for the $K_{\alpha 2}$ x-ray gate in the (L x ray)($K_{\alpha 2}$ x ray) coincidence runs. This is of particular significance in view of the fact that the false coincidences are contributed by $K_{\alpha 1}$ x-ray events present in the gate. Figure 8 shows the position of the window on $K_{\alpha 2}$ x rays. The shape of the $K_{\alpha 1}$ x ray is drawn by comparison with that of the 60-keV line from Am^{241}. The shaded portion in the figure indicates the $K_{\alpha 1}$ contamination. In a typical run, the composition of the $K_{\alpha 2}$ gate is $C_{K_{\alpha 2}}:C_{K_{\alpha 1}}:C_{K_\beta}=0.90:0.05:0.05$.

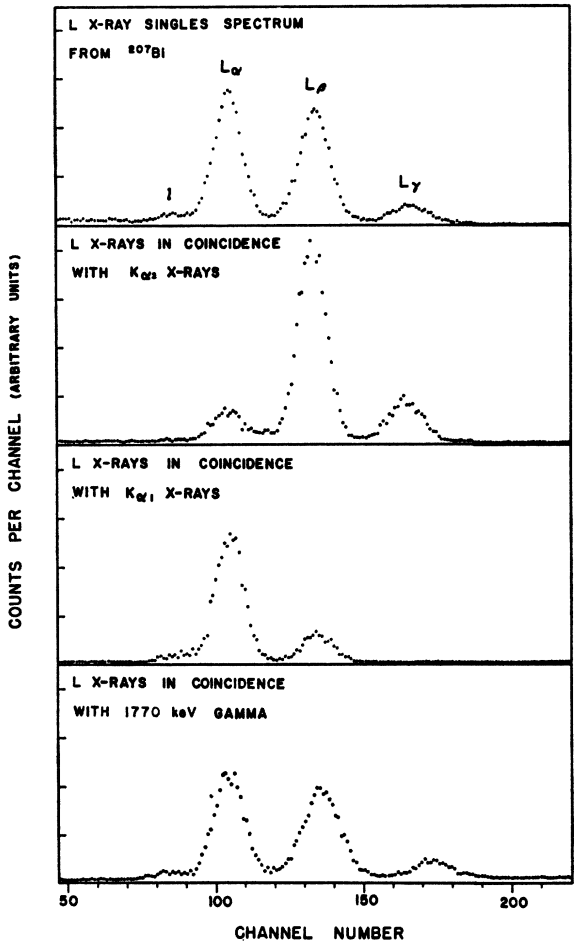

FIG. 5. Typical L-x-ray spectra taken with the Si(Li) x-ray spectrometer. The presence of L_α components in ccincidence with $K_{\alpha 2}$ x rays demonstrates the Coster-Kronig transfer of vacancies from the L_2 to the L_3 subshell.

The coincidence efficiency ϵ_c of the system was calibrated by measuring the coincident K-x-ray spectrum gated by 136-keV γ rays from a Co^{57} source. The coincidence rate $C_{K(\gamma)}$ is related to the coincidence efficiency ϵ_c by the relation

$$C_{K(\gamma)}=C_{(\gamma)}P_K\omega_K\epsilon_K\Omega_K f_K\epsilon_c, \tag{13}$$

where ϵ_K, Ω_K, and f_K are quantities for K x rays, as defined in Eq. (1); ω_K is the K-fluorescence yield of iron (0.319).[1] The value of the K-capture probability P_K for Co^{57} decay was taken as 0.885.[8] The coincidence efficiency was found to be unity for the fast coincidence resolving times employed. A further verification of $\epsilon_c=1.0$ was made by performing a slow coincidence experiment with resolving time $2\tau=7$ μsec. Some of the earlier coincidence runs also were performed using a conventional fast coincidence system described elsewhere.[17]

The two detectors were positioned at 135° to each other for all of the coincidence measurements in the present work.

III. RESULTS

The results obtained in the present work are summarized below.[19] Table III presents the relative intensities of all x rays and γ rays emitted in the decay of Bi^{207} from present investigations. Figure 9 shows the revised decay scheme of Bi^{207} where the percentage branchings are obtained by assuming theoretical conversion coefficients from Hager and Seltzer.[9] Table IV presents the relative intensities of L_α, L_β, and L_γ x-ray components from the L_2 and L_3 subshells, together with literature values.

Table V lists the L-subshell fluorescence and Coster-Kronig yields, along with values from the literature. A value of $s_1=0.433$ is assumed from the work of Goldberg[15] in evaluating f_{13}, f_{12}, and ω_1[Eqs. (11) and (12)].

The quoted standard errors include those due to statistics, detector efficiency, solid angles, and attenuation corrections. Errors in counting statistics were less than 1%. In L-K_α x-ray coincidences, the estimated L x rays from other coincident transitions in cascade were found to be negligible. The values quoted are averages of several sets of measurements in each case.

IV. DISCUSSION

Our value of ω_3 is lower than all previous measurements.[1,14] Angular-correlation effects between the L

[19] Some of the results were presented in a preliminary report at the *Proceedings of the International Conference on Electron Capture and Higher Order Processes in Nuclear Decay* (Kultura Bookexport, Budapest, Hungary, 1968).

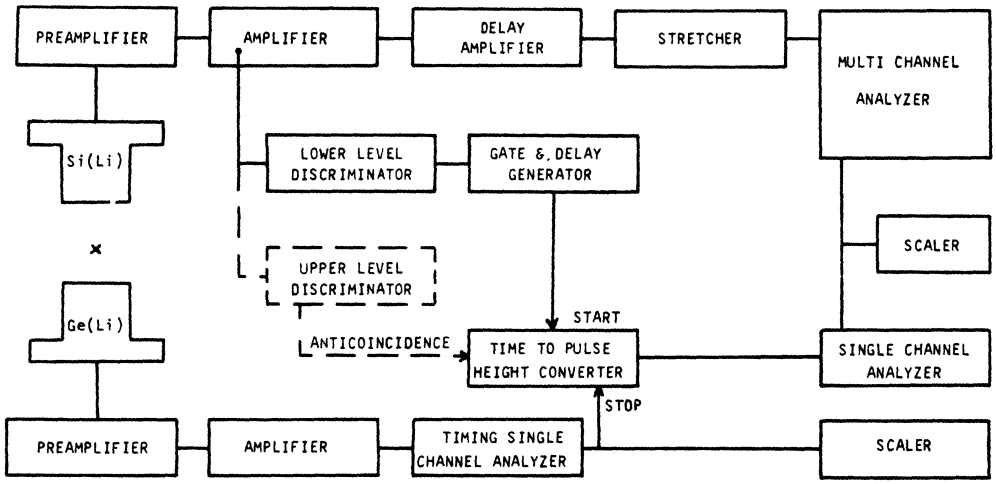

FIG. 6. Block diagram of the coincidence spectrometer.

and K x rays following K-shell ionization has not been taken into account in the present work. Recent experimental studies, however, indicate that a correlation exists. Beste[20] has found that the ratio $\omega_{KL}(90°)/\omega_{KL}(180°)$ is 0.09 ± 0.06 for lanthanum ($Z=57$). Price *et al.*[4] measured the same ratio with high-resolution techniques for five elements in the range of $Z=73$–91 and found that no correlation exists in the case of the L_2 subshell, as expected, while in the case of the L_3 subshell, $\omega_3(90°)$ is definitely lower than $\omega_3(180°)$. These authors also gave theoretical estimates for this ratio as 0.059 and 0.044 in the case of the L_3 subshell. If the effect of angular correlation is included, the value of ω_3 will thus be increased at most by 6% to a value of 0.334. This value is in agreement with the semitheoretical estimates of Listengarten.[21] The recent measurement of ω_3 for $Z=83$ (0.345 ± 0.018) by Freund and Fink,[22] using singles L-x-ray spectra (a method which is free of the angular-correlation effects), also gives a value lower than earlier data.

There is excellent agreement with the work of Price *et al.*[4] in the case of ν_2. The other two earlier values of ν_2 listed in Table V are from poor resolution experiments.

The only other previous experimental information on the L_1 subshell is the value of ω_{LL} (0.36 ± 0.02) from Jopson, Mark, and Swift.[23] The value of ν_1 calculated from this value turns out to be 0.355. The four coincidence experiments in the present work with different vacancy distributions yielded a consistently lower value for ν_1. An average of these four values is adopted, $\nu_1=0.295\pm0.010$.

The present work conclusively demonstrates that the vacancies are transferred from the L_2 to the L_3 subshell, as seen in Fig. 5, from the presence of L_α x rays in coincidence with $K_{\alpha 2}$ x rays. This is in agreement with the earlier work of Rao and Crasemann on Ta and Hg.[2] A large number of earlier measurements of L-subshell fluorescence yields and Coster-Kronig yields were based on the assumption that $f_{23}=0$ and therefore

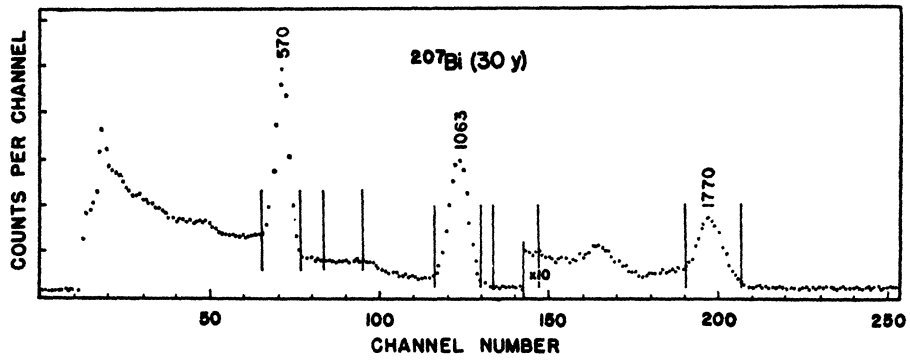

FIG. 7. The γ-ray spectrum from Bi^{207} decay taken with a 7.5×7.5-cm NaI(Tl) detector. The positions of the SCA windows selecting the γ-ray gates in the L-x-ray–γ-ray coincidence measurements are shown.

[20] H. W. Beste, Z. Physik **213**, 333 (1968).
[21] M. A. Listengarten, Izv. Akad. Nauk SSSR, Ser. Fiz. **24**, 1041 (1960) [English transl.: Soviet Phys.—Bull. Acad. Sci. USSR, Phys. Ser. **24**, 1050 (1960)].
[22] H. U. Freund and R. W. Fink, this issue, Phys. Rev. **178**, 1952 (1969).
[23] R. C. Jopson, Hans Mark, and C. D. Swift, Phys. Rev. **128**, 2671 (1962).

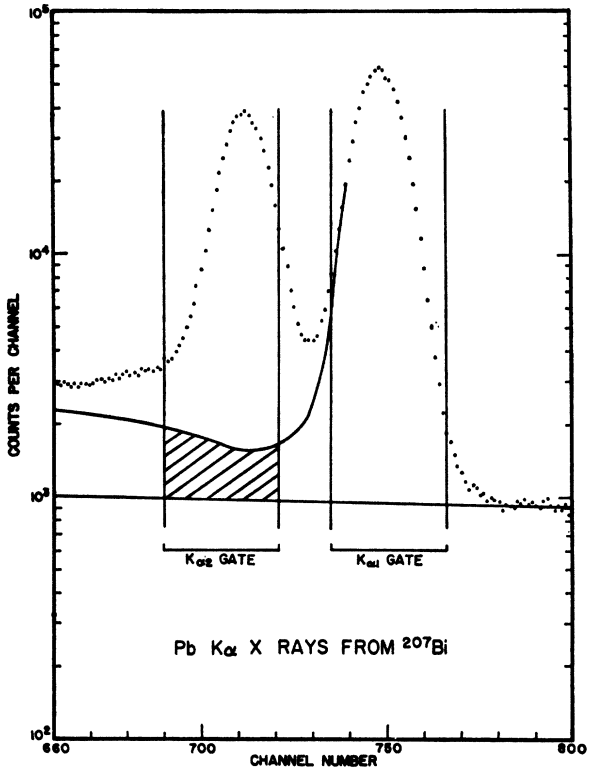

FIG. 8. The positions of the SCA window selecting the $K_{\alpha 1}$ and $K_{\alpha 2}$ x-ray gates in a typical run are shown. The shape of the $K_{\alpha 1}$ x-ray peak is derived from that of a monoenergetic γ ray. The cross-lined portion indicates the contribution of $K_{\alpha 1}$ x rays to the $K_{\alpha 2}$ x-ray gate.

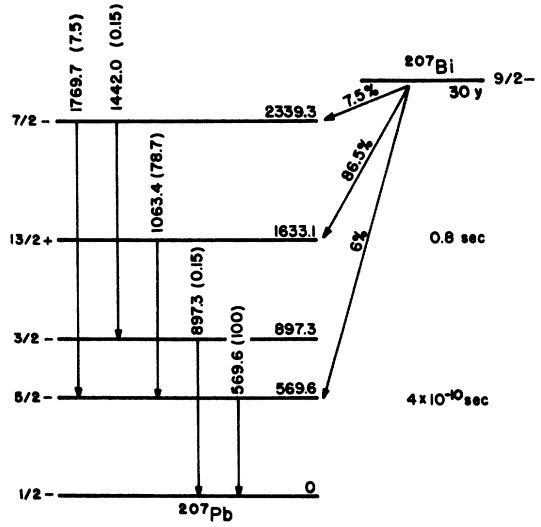

FIG. 9. Revised decay scheme of Bi^{207} decay.

TABLE III. Relative intensities of x rays and γ rays in Bi^{207} decay.

Radiation (keV)	Relative intensities
L x rays[a]	35.0±2.0
K x rays	79.5±4.0
569.6-keV γ ray	100
897.3-keV γ ray	0.150±0.015
1063.4-keV γ ray	78.7±4.0
1442.0-keV γ ray	0.150±0.015
1769.7-keV γ ray	7.5±0.4

[a] $L_l : L_\alpha : L_\beta : L_\gamma = 5.5 : 43.5 : 42.4 : 8.6$.

TABLE IV. Relative intensities of L-x-ray components from the L_2 and L_3 subshells directly.

	L_2 subshell			L_3 subshell		
	$L_{l\alpha}$	L_β	L_γ	$L_{l\alpha}$	L_β	L_γ
Present work	0	1	0.248±0.019	1	0.223±0.017	0
Goldberg[a]	0	1	0.371	1	0.257	0

[a] Reference 15.

TABLE V. Pb L-subshell fluorescence yields and Coster-Kronig transition probabilities.

	Present work	Previous work
L_1 subshell		
ν_1	0.295±0.010	0.355[a]
ω_1	0.07±0.02	0.37[b]
f_{12}	0.15±0.04	
f_{13}	0.57±0.03	
L_2 subshell		
ν_2	0.417±0.015	0.264,[c] 0.50,[d] 0.410[e]
ω_2	0.363±0.015	0.24,[b] 0.354[e]
f_{23}	0.164±0.016	
L_3 subshell		
ω_3	0.315±0.013	0.35,[b] 0.337,[c] 0.35,[d] 0.354,[e] 0.32[f]

[a] Calculated from $\omega_{LL}=0.36$ in Ref. 22.
[b] Quoted in Ref. 1.
[c] H. Küstner and E. Arends, Ann. Physik **22**, 443 (1935).
[d] Reference 3.
[e] Reference 4.
[f] R. J. Stephenson, Phys. Rev. **51**, 637 (1937).

need to be revised.[1,14] Price *et al.*[4] have calculated ω_2 from their values of ν_2 assuming a constant value of $f_{23}=0.13$ in the range $Z=70$–92. The possible variation in f_{23} with Z is to be taken into consideration and further experimental and theoretical work on f_{23} is necessary to improve the situation.

The Coster-Kronig transition probabilities f_{12} and f_{13} are not very well known. There are a large number of experimental estimates for Z around 80. Listengarten[21] has estimated f_{ij} versus Z curves based on the radiation, Auger, and Coster-Kronig widths and normalized them to available experimental data. The present values of $\omega_1=0.07\pm0.02$, $f_{12}=0.15\pm0.04$, and $f_{13}=0.57\pm0.03$ are in reasonable agreement with these curves.

Using high-resolution singles L-x-ray spectra, together with recent precision L-conversion and L Auger electron absolute intensities, Freund and Fink[22] obtained a value of $\omega_1=0.095\pm0.005$ at $Z=83$, which compares well with the present value for $Z=82$.

ACKNOWLEDGMENTS

The authors should like to express their appreciation to L. A. Rauber for laboratory assistance. They are also grateful to Professor L. D. Wyly for the loan of a Bi^{207} source.

PHYSICAL REVIEW VOLUME 178, NUMBER 4 20 FEBRUARY 1969

Nuclear Structure of Pb^{205} from the (d, t) Reaction*

ROBERT TICKLE AND JOHN BARDWICK

Cyclotron Laboratory, Department of Physics, The University of Michigan, Ann Arbor, Michigan 48105

(Received 18 October 1968)

The structure of Pb^{205} has been investigated using the neutron pickup reaction $Pb^{206}(d, t)Pb^{205}$ at a bombarding energy of 21.6 MeV. A distorted-wave analysis (DWA) has been made of the angular distributions of seven triton groups that excite ten levels in Pb^{205}. The spectrum is sparse; most of the strength corresponding to pickup from a given orbital in the target is contained in a single level. Configuration assignments and spectroscopic factors derived from the DWA are found to agree well with a shell-model calculation of the structure of Pb^{205} by Miranda.

I. INTRODUCTION

DURING the past several years, there has been a rapid accumulation of nuclear spectroscopic data in the lead region of the periodic table. It is now apparent that the nuclei around lead can be described fairly well by the shell model. This has been demonstrated, for example, by comparisons[1–3] of shell-model calculations with the level structures of Pb^{208}, Pb^{206}, and Bi^{208}. These comparisons have emphasized the good agreement between experiment and theory. Also, the results obtained from the many experiments that have studied the excitation of isobaric analog states in this region have been, for the most part, successfully interpreted in terms of the shell model.

The level structure of Pb^{205} is of interest because the low-lying levels should be described, according to the shell model, in terms of three-neutron-hole configurations. With only three holes, the structure of Pb^{205} can be calculated and will afford us an opportunity to make a detailed comparison between experiment and theory for another nucleus in this region—a region of exceptional current interest for nuclear spectroscopic studies. Considerable experimental data exist in the literature which help to establish the energy levels in Pb^{205}. These include accurate measurements of the γ-ray energies[4–7] in the spectrum following the decay of excited states in Pb^{205}, triton spectra from the $Pb^{206}(d, t)Pb^{205}$ reaction,[8] and a study of the $Pb^{204}(d, p)Pb^{205}$ reaction including angular distributions.[9]

In the following sections we report the results of an experimental study of the structure of Pb^{205} using the neutron pickup reaction $Pb^{206}(d, t)Pb^{205}$. The purpose of this study was to augment present knowledge of Pb^{205} by measuring triton angular distributions and extracting from these data l values and spectroscopic factors. The ground-state wave function of Pb^{206} is known from experiment.[2,8] It is therefore possible to calculate theoretical spectroscopic factors from shell-

* Supported in part by the U.S. Atomic Energy Commission.

[1] J. Bardwick and R. Tickle, Phys. Rev. **161**, 1217 (1967).

[2] R. Tickle and J. Bardwick, Phys. Rev. **166**, 1167 (1968).

[3] W. P. Alford, J. P. Schiffer, and J. J. Schwartz, Phys. Rev. Letters **21**, 156 (1968).

[4] C. J. Herrlander, Arkiv Fysik **20**, 71 (1961).

[5] I. Bergstrom, C. J. Herrlander, P. Thieberger, and J. Uhler, Arkiv Fysik **20**, 93 (1961).

[6] E. T. Jurney, H. T. Motz, and S. H. Vegors, Jr., Nucl. Phys. **A94**, 351 (1967).

[7] S. H. Vegors, R. L. Heath, and D. G. Proctor, Nucl. Phys. **48**, 230 (1963).

[8] P. Mukherjee and B. L. Cohen, Phys. Rev. **127**, 1284 (1962); B. L. Cohen, R. E. Price, and S. Mayo, Nucl. Phys. **20**, 360 (1960).

[9] J. H. Bjerregaard, O. Hansen, and O. Nathan, Nucl. Phys. **A94**, 457 (1967).